Laser and Particle Beams

cambridge.org/lpb

Oscillating two-stream instability in strongly coupled plasma

Prerana Sharma, K. Avinash and D. N. Gupta

Department of Physics and Astrophysics, University of Delhi, Delhi 110007, India

Research Article

Cite this article: Sharma P, Avinash K, Gupta DN (2018). Oscillating two-stream instability in strongly coupled plasma. *Laser and Particle Beams* **36**, 376–383. https://doi.org/10.1017/S0263034618000368

Received: 20 February 2018
Revised: 26 February 2018
Accepted: 23 August 2018

Key words:
Inertial confinement fusion; laser-driven ion acceleration; oscillating two-stream instability; strongly coupled plasma

Author for correspondence:
Prerana Sharma, Department of Physics and Astrophysics, University of Delhi, Delhi 110007, India. E-mail: preranasharma4@gmail.com

Abstract

Oscillating two-stream instability (OTSI) of a high amplitude laser or a plasma wave is investigated in plasmas with strongly coupled ions. It is shown that in some parameter regime, the pressure of strongly coupled ions becomes negative, which leads to enhance the bunching of ion and concomitant destabilization of OTSI. Applications of these results to ion accelerator and inertial confinement fusion experiments are discussed.

Introduction

In inertial confinement fusion (ICF) and laser-driven ion accelerator, high power laser interacts with a solid target (Snavely *et al.*, 2000; Lindl *et al.*, 2014). When the laser beam comes into contact with the outer surface of this target, plasma is created due to ionization of target atoms by the electric field of the laser. This plasma expands outward from the surface. The density of this laser produced plasma is spatially inhomogeneous. Laser plasma instabilities (LPI) occur at different density region in this inhomogeneous plasma (Rosenbluth, 1972; Weaver *et al.*, 2007), for example, parametric decay instability (PDI) occurs at the region where laser frequency (ω_0) is greater than local plasma frequency (ω_{pe}), while oscillating two-stream instability (OTSI) occurs in the denser region where ω_0 is $\leq\omega_{pe}$ (Chen, 1985; Liu and Tripathi, 1995).

In direct drive experiments (Craxton *et al.*, 2015), this interaction occurs in the outer corona which is made of carbon and hydrogen ions. While in indirect drive experiments (Lindl *et al.*, 2004), these instabilities occur in the low Z H/He plasma and high Z Au blow-off plasma in the vicinity of hohlraum wall. In the blow-off plasma near the Au hohlraum wall, the ion species is mostly due to high Z Au ions. The typical density of these ions is in the range $n_i \leq 10^{21}$ cm^{-3} ($n_{cr} \approx 10^{22}$ cm^{-3} for $\lambda_{\text{laser}} \approx 351$ nm, n_{cr} is the critical density), the ion temperature T_i is typically in the range 5–50 eV and $Z \approx 10-20$ (for Au ions). Under these conditions, Sharma *et al.* (2016) have shown the ratio of typical electrostatic potential energy to typical kinetic energy of Au ions is >1, that is, $\Gamma_i = (Z^2e^2/a_iT_i) > 1$; where Γ_i is the ion coupling parameter and a_i ($= (3/4\pi n_i)^{1/3}$) is the mean distance between ions. Thus the high Z Au ions may become strongly coupled. These instabilities can also occur in plasma relevant to laser-driven ion accelerator near the target surface (Wilks *et al.*, 2001; Esirkepov *et al.*, 2014). In this process, a thin target foil (hydrogen, carbon or aluminum) is irradiated by an intense laser pulse. The laser prepulse creates a preplasma on the target's front side, where the density of plasma is near critical density (Esirkepov *et al.*, 2014). The main pulse interacts with the plasma and accelerates a part of target electrons, mainly in the forward direction. The electrons so accelerated create charge separation. The charge separation provides a strong electric field by which the target ions are accelerated. This ion acceleration mechanism is called as target normal sheath acceleration (Wilks *et al.*, 2001). The typical target ions can be hydrogen, carbon, oxygen or aluminum. In this case, the plasma density is close to the critical density n_{cr}, Z is ≈ 5–10 (for Al ion) and the temperature of the ions is in the range 10–100 eV, hence the ions may become strongly coupled in the preplasma. For example, with ion density in the range $n_i \approx 10^{21}$ cm^{-3}, the mean particle distance a_i is $\approx 6\times10^{-8}$ cm. Then for Al ions with temperature $T_i \approx 30$ eV and $Z = 9$, the ion coupling parameter, $\Gamma_i = (Z^2e^2/a_iT_i) \approx 7$. The electrons are still weakly coupled due to smaller charge and higher temperature, as for $T_e \approx 50-500$ eV and $Z = 1$, $\Gamma_e < 1$.

Extensive studies related to LPI have been done by various authors in the weakly coupled plasma. Kirkwood *et al.* (1996) have reported experimental results on stimulated Raman scattering (SRS) and stimulated Brillouin Scattering (SBS) from Xe plasma embedded with C_5H_{12}impurities. Fernandez *et al.* (1996) have observed the dependence of SRS on ion acoustic damping in hohlraum plasmas. Yadav *et al.* (2003) have studied SBS of a laser in a high-Z plasma channel embedded with light ions. Satya *et al.* (1985) obtained the analytical reductions of the low-frequency dispersion relation of the field- plasma system, including results on the OTSI. Kumar and Malik (2006) studied the effect of negative ions on OTSI of laser-driven plasma beat wave in homogeneous plasma. All the above-mentioned studies of plasma

© Cambridge University Press 2018

CAMBRIDGE UNIVERSITY PRESS

instabilities containing high Z ions have been done in the weakly coupled plasma, that is, $\Gamma_{i,e}$ <1. In addition, other types of instabilities have been studied in different types of plasma models (Malik and Singh, 2011; Singh *et al.*, 2013; Malik *et al.*, 2015*a*; 2015*b*; Tyagi *et al.*, 2018).

In recent years, a great deal of attention has been focused on different plasma instabilities in strongly coupled plasma also. Janaki *et al.* (2011) studied Jeans instability in a viscoelastic gravitational fluid. Das and Kaw (2014) have studied the suppression of Rayleigh Taylor instability in strongly coupled plasmas. Sharma *et al.* (2016) studied the parametric instabilities (stimulated Brillouin scattering, PDI, and Langmuir decay instability) in laser plasmas with strongly correlated/coupled ions. In this paper, we study the OTSI of a high power laser in plasma where ions are strongly coupled. OTSI is an important non-linear process in a high power laser–plasma interaction near the critical layer (Fried *et al.*, 1976; Nicholson, 1981; Mulser *et al.*, 1984). In this process, a laser or a long wavelength plasma wave decays into a low-frequency mode and two Langmuir wave sidebands. In uniform plasma, the low-frequency mode turns out to be purely growing with time and the growth rate is less than or comparable with the ion plasma frequency. OTSI of a laser in two ion species plasma was shown by Yadav *et al.* (2004). Malik (2007) investigated OTSI in a negative ion containing plasma with hot and cold positive ions and found that the effects of charge number and mass of the ions are significant on the instability. But OTSI in strongly coupled plasma has not been studied yet.

In the strongly coupled regime, the ion fluid behaves like a strongly coupled visco-elastic fluid (Frenkel, 1946; Boon and Yip, 1980). In our paper, we take into account these strong coupling effects *via* generalized hydrodynamic (GHD) equation for ions (Berkovsky, 1992; Kaw and Sen, 1998; Murillo, 1998). In this equation, the strong coupling effects are parameterized by a typical relaxation time $\tau_m(\Gamma_i)$. For $\tau_m = 0$ there are no memory effects and the GHD equation reduces to the standard Navier Stokes equation for viscous medium. On the other hand in the limit $\tau_m \to \infty$ memory effects persist and the medium acquires solid like elastic properties. In the range $0 < \tau_m < \infty$, the medium has viscous as well solid like elastic properties that is, viscoelastic fluid. Electrons are still weakly correlated. It should also be noted that in this parameter regime, the electrons and the ions, both are well within the non-degenerate regime. This phenomenon is of relevance to studies of plasma heating, ICF and laser-driven ion accelerator.

The paper is organized as follows in the section Governing equations the governing equations for strongly coupled ions and weakly coupled electrons are discussed. In the section Oscillating two-stream instability the effects of the strong correlation of ions on OTSI has been studied. The last section summarizes the conclusion.

Governing equations

In our model, we consider strongly coupled ions. These ions could be either the high Z Au ions in the blow-off plasma near the vicinity of hohlraum or the Al ions in the preplasma of the target front in laser-driven ion accelerator. The dynamics of the strongly coupled ions is described by GHD equation given by

$$\frac{d\,\vec{v}_i(\vec{r},t)}{dt} + \frac{\nabla P_i(\vec{r},t)}{n_i m_i} + \frac{Ze\nabla\varphi(\vec{r},t)}{m_i} = \int_{-\infty}^{t} dt' \int dr' \eta_i(\vec{r}-\vec{r}', t-t')\vec{v}_i(\vec{r}', t'), \quad (1)$$

where $d/dt = (\partial/\partial t + \vec{v}_i \cdot \nabla)$, $\vec{v}_i$ is the ion fluid velocity, P_i is the ion pressure, m_i is mass of the ion, n_i is ion density, φ is the electrostatic potential, $Z = q_i/e$, q_i is the charge on multiple charged Au or Al ion, e is the electronic charge and η_i is a non-local ion viscoelastic operator (as defined in the section Oscillating two-stream instability). The continuity equation for ions is given by

$$\frac{\partial n_i}{\partial t} + \nabla \cdot (n_i \vec{v}_i) = 0. \quad (2)$$

Eqs. (1) and (2) will be used to calculate the ion susceptibility with strong correlation effects. The electron fluid is weakly coupled which is governed by following a set of equations

$$\frac{\partial n_e}{\partial t} + \nabla \cdot (n_e \vec{v}_e) = 0, \quad (3)$$

$$n_e m_e \frac{d\vec{v}_e}{dt} = e n_e \nabla\varphi - e n_e \frac{\vec{v}_e \times \vec{B}}{c} - \nabla P_e, \quad (4)$$

where $d/dt = (\partial/\partial t + \vec{v}_e \cdot \nabla)$, $\vec{B}$ is magnetic field, m_e is mass of electron, $P_e$is the electron pressure and n_e, $\vec{v}_e$ are electron number density and velocity, respectively. These equations are supplemented with the set of Maxwell's equations.

$$\nabla \cdot \vec{E} = 4\pi e(Zn_i - n_e), \nabla \times \vec{E} = -\frac{1}{c}\frac{\partial \vec{B}}{\partial t}, \nabla \times \vec{B} = \frac{4\pi}{c}\vec{J} + \frac{1}{c}\frac{\partial \vec{E}}{\partial t}, \nabla \cdot \vec{B} = 0, \quad (5)$$

where $\vec{J} = e(Zn_i\vec{v}_i - n_e\vec{v}_e)$ is the net plasma current density.

Oscillating two-stream instability

In OTSI a long wavelength laser pump wave excites short wavelength electrostatic waves and a low-frequency mode which is a purely growing density perturbation. The physics of this instability is as follows (Chen, 1985). Consider a quasi-neutral density perturbation in plasma as shown in Figure 1. In case when pump frequency ω_0 is less than ω_{pe}, which is the resonant frequency of cold electron fluid, electrons move opposite to the direction of laser electric field. Since ions do not respond on the high-frequency time scale, an electric field is created due to the charge separation. The ponderomotive force ($\vec{F}_p$) due to this electric field creates a bunching of ions which causes OTSI. The pressure gradient of electrons and ions oppose the tendency of bunching which results in the threshold of OTSI. We will show later, that the ion pressure gets modified due to the strong coupling effects. It decreases with Γ_i and in certain parameter regime (Γ_i >4) it becomes negative. Ion bunch collapse under this negative pressure as shown in Figure 1 thereby leading to significant enhancement of ion bunching and destabilization OTSI.

Consider a laser pump (ω_0, $\vec{k}_0$) decays into two sideband waves ($\omega_{a,b}$, $\vec{k}$) and one low frequency (ω, $\vec{k}$) mode density perturbation where $\omega_{a,b} = \omega \mp \omega_0$ and $\vec{k}_0 \approx 0$. Here (ω, $\vec{k}$) may not be an eigenmode of the system; it could be a driven mode. However, the sidebands are the Langmuir eigenmodes within a slight frequency mismatch due to nonlinear coupling. The dipole laser pump field is taken to be coherent given by $\vec{E}_0 = \hat{z}A_0 e^{-i\omega_0 t}$

https://doi.org/10.1017/S0263034618000368 Published online by Cambridge University Press

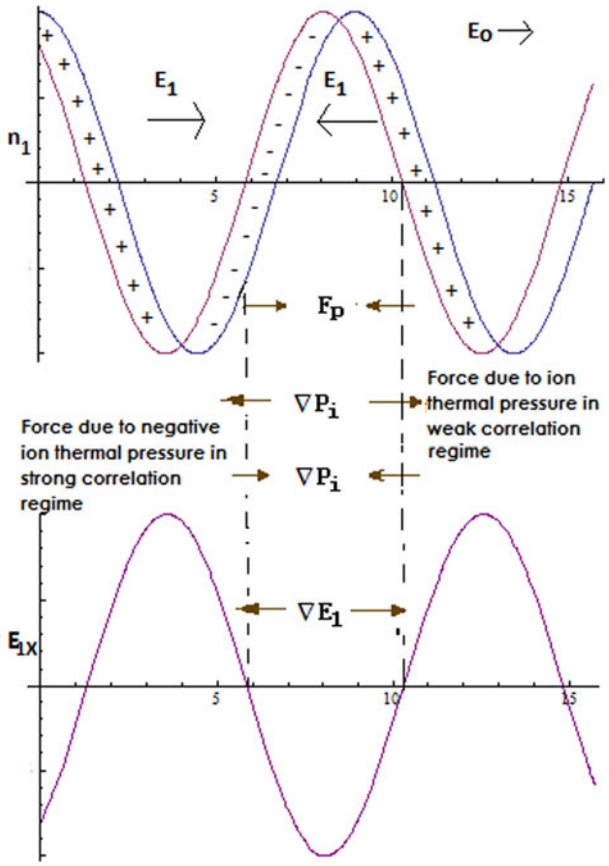


Fig. 1. Physical mechanism of OTSI in weakly and strongly coupled plasma.

with $\omega_0 \approx \omega_{pe}$. The electrostatic potentials are

$$\varphi_l = Ae^{-i(\omega t - \vec{k}\cdot\vec{r})}, \tag{6}$$

$$\varphi_{a,b} = A_{a,b}e^{-i(\omega_{a,b}t - \vec{k}\cdot\vec{r})}. \tag{7}$$

The perturbed equation of motion for electron fluid is

$$n_{e0}m_e\left(\frac{\partial\vec{v}_{e1}}{\partial t} + \vec{v}_{e1}\cdot\nabla\vec{v}_{e1}\right) = -en_{e0}(\vec{E}_0 - \nabla\varphi) - \nabla P_{e1}. \tag{8}$$

The perturbed electron continuity equation is

$$\frac{\partial n_{e1}}{\partial t} + n_{e0}\nabla\cdot\vec{v}_{e1} + \nabla\cdot\left(\frac{1}{2}n_{e1}\vec{v}_{e1}\right) = 0, \tag{9}$$

where $\vec{v}_{e1}$, P_{e1}, n_{e1}, φ are the perturbed electron velocity, pressure, density, and the electric potential, respectively, and n_{e0} is the equilibrium electron density. Here the electrons will contribute to both, the high-frequency part and the low-frequency part. The high-frequency part corresponds to the laser (ω_0) and sidebands (ω_a, ω_b) where electrons move independently of ions and the low-frequency part corresponds to the low-frequency mode (ω)where the electrons move along with ions in quasi-neutral manner. Hence for the electrons the quantities $\vec{v}_{e1}$, P_{e1}, n_{e1}, and φ each contains a high-frequency part ($\vec{v}_{e0}$, $\vec{v}_{ea,b}$, $P_{ea,b}$, $\varphi_{a,b}$, and $n_{ea,b}$) and a low-frequency part ($\vec{v}_{el}$, P_{el}, φ_l, and n_{el}).

To the lowest order of Eq. (8), the motion in response to high-frequency laser electric field E_0 is

$$\frac{\partial\vec{v}_{e0}}{\partial t} = -\frac{e\vec{E}_0}{m_e} \tag{10}$$

This gives the electron oscillatory velocity $\vec{v}_{e0} = \dfrac{e\vec{E}_0}{m_e i\omega_0}$.

For the high-frequency sidebands, the equation of motion for electron fluid is-

$$m_e\frac{\partial\vec{v}_{ea,b}}{\partial t} = e\nabla\varphi_{a,b} - \frac{\nabla P_{ea,b}}{n_{e0}}, \tag{11}$$

where $\vec{v}_{ea,b}$, $n_{ea,b}$, $\varphi_{a,b}$, and $P_{ea,b}$ correspond to the high-frequency part at $\omega_{a,b}$, $\vec{k}$. The oscillatory velocities of electrons correspond to sideband waves (neglecting the pressure term) will be

$$\vec{v}_{ea,b} = -\frac{e\vec{k}}{m_e\omega_{a,b}}\varphi_{a.b}. \tag{12}$$

In the low-frequency part, the sidebands, and the pump wave beat and produce a low-frequency ponderomotive force $\vec{F}_p$ on electrons as $\omega = \omega_{a,b} \pm \omega_0$. Hence the equation of motion for low-frequency electrons along with the ponderomotive force is given by

$$m_e\left(\frac{\partial\vec{v}_{el}}{\partial t} + \vec{v}_{e0}\cdot i\vec{k}\vec{v}_{ea} + \vec{v}^{*}_{e0}\cdot i\vec{k}\vec{v}_{eb}\right) = e\nabla\varphi_l - \frac{i\vec{k}n_{el}T_e}{n_{e0}}, \tag{13}$$

where $\vec{v}_{el}$, n_{el}, and φ_l correspond to low-frequency part and T_e is the electron temperature. The ponderomotive force $\vec{F}_p$ can be defined as

$$\vec{F}_p = e\nabla\varphi_p = -(m_e/2)\nabla(\vec{v}_{e0}\cdot\vec{v}_{ea} + \vec{v}^{*}_{e0}\cdot\vec{v}_{eb}). \tag{14}$$

This gives the ponderomotive potential

$$\varphi_p = \frac{\vec{k}\cdot\vec{v}_{e0}}{2\omega_a}\varphi_a + \frac{\vec{k}\cdot\vec{v}^{*}_{e0}}{2\omega_b}\varphi_b. \tag{15}$$

Using Eqs. (14) and (15) in Eq. (13) we get

$$m_e\frac{\partial\vec{v}_{el}}{\partial t} = e\nabla(\varphi_l + \varphi_p) - \frac{i\vec{k}n_{el}T_e}{n_{e0}}. \tag{16}$$

The low-frequency part of Eq. (9) gives

$$\frac{\partial n_{el}}{\partial t} + n_{e0}i\vec{k}\cdot\vec{v}_{el} = 0. \tag{17}$$

Using Eqs. (16) and (17) we can find the low-frequency electron density perturbation which is due to the ponderomotive and self-consistent potential φ_p and φ_l

$$n_{el} = \frac{k^2}{4\pi e}\chi_e(\varphi_l + \varphi_p), \tag{18}$$

where χ_e is the low-frequency electron susceptibility at ω, k. For $\omega \ll kv_{th}$ ($v_{th} = (2T_e/m_e)^{1/2}$ is electron thermal speed),

https://doi.org/10.1017/S0263034618000368 Published online by Cambridge University Press

$\chi_e \approx 2\omega_{pe}^2/k^2v_{th}^2 = \omega_{pi}^2/k^2C_{s0}^2$ (where $\omega_{pi} = ((4\pi n_{i0}Z^2e^2)/m_i)^{1/2}$is ion plasma frequency and $C_{S0} = (ZT_e/m_i)^{1/2}$). The equation of motion of strongly coupled ion fluid is obtained by linearizing Eq. (1) as

$$\frac{\partial \vec{v}_{i1}(\vec{r},t)}{\partial t} + \frac{\nabla P_{i1}(\vec{r},t)}{n_{i0}m_i} + \frac{Ze\nabla\varphi_l(\vec{r},t)}{m_i} = \int_{-\infty}^{t} dt' \int dr' \eta_i(\vec{r}-\vec{r}', t-t')\vec{v}_{i1}(\vec{r}', t'), \tag{19}$$

where $\vec{v}_{i1}$, P_{i1}, φ_l are the perturbed ion velocity, pressure and the electric potential, respectively, and n_{i0} equilibrium ion density. The quantity η_i may be identified as a nonlocal viscoelastic operator (Berkovsky, 1992; Kaw and Sen, 1998) which accounts for memory effects and for the short-range order that begins to develop in the plasma as a result of the growing correlation between the ions with increasing values of Γ_i. If the memory function is regarded as a simple exponential function with τ_m as the relaxation time, then the Fourier transform of η_i can be expressed as (Kaw and Sen, 1998)

$$\eta_i(\omega, k) = \frac{\eta k^2 + \left(\frac{\eta}{3} + \zeta\right)\vec{k}(\vec{k}\cdot)}{m_i n_{i0}(1 - i\omega\tau_m)}, \tag{20}$$

where ω and k are the frequency and the wave number of the low-frequency mode, η, ζ are shear and bulk viscosities. Combining Eqs. (19) and (20) we can express the GHD equation as

$$\left[1 + \tau_m\frac{\partial}{\partial t}\right]\left[m_i n_{i0}\frac{\partial \vec{v}_{i1}}{dt} + Zen_{i0}\nabla\varphi_l + \nabla P_{i1}\right] = \eta\nabla\cdot\nabla\vec{v}_{i1} + \left(\zeta + \frac{\eta}{3}\right)\nabla(\nabla\cdot\vec{v}_{i1}). \tag{21}$$

Linearizing the ion continuity equation given by Eq. (2)

$$\frac{\partial n_{i1}}{\partial t} + n_{i0}i\vec{k}\cdot\vec{v}_{i1} = 0. \tag{22}$$

The ion density perturbation n_{i1} can be obtained by using Eq. (22) to eliminate the perturbed velocity in Eq. (21) which gives

$$n_{i1} = -\frac{k^2}{4\pi Ze}\chi_i\varphi_l, \tag{23}$$

where χ_i is the ion susceptibility such that

$$\chi_i = -\frac{\omega_{pi}^2}{\left[\omega^2 - \gamma_i\mu_i k^2 v_{thi}^2 + \frac{i\omega\eta^* k^2 a_i^2\omega_{pi}}{(1 - i\omega\tau_m)}\right]}, \tag{24}$$

where $\gamma_i = C_{pi}/C_{vi}$ is an adiabatic index, $v_{thi} = (2T_i/m_i)^{1/2}$ is the ion thermal velocity, $\mu_i(\Gamma_i) = (1/T_i)(\partial P_i/\partial n_i)_{T_i} = 1 + u(\Gamma_i)/3 + (\Gamma_i/9)\partial u(\Gamma_i)/\partial\Gamma_i$ is compressibility (Ichimaru *et al.*, 1987) and $u(\Gamma_i)$ is the normalized excess internal energy. For weakly coupled plasma ($\Gamma_i < 1$), $u(\Gamma_i) \approx -\sqrt{3}/2\ \Gamma_i^{3/2}$ and for $1 \le \Gamma_i \le 200$, Slattery *et al.* (1980; 1982) have given the empirical relation- $u(\Gamma_i) = -0.89\Gamma_i + 0.95\Gamma_i^{1/4} + 0.19\Gamma_i^{-1/4} - 0.81$. For weak coupling ($\Gamma_i \approx 0$) the value of $\mu_i = 1$. As we increase Γ_i the value of μ_i decreases, goes to 0 for $\Gamma_{cr} \approx 3$ and becomes negative for $\Gamma_i > \Gamma_{cr}$. Here τ_m and η^* are given by

$$\tau_m = \frac{\eta^*}{\omega_{pi}\lambda_i^2}\frac{a_i^2}{1 - \gamma_i\mu_i + \frac{4}{15}u(\Gamma_i)} \tag{25a}$$

$$\eta^* = \frac{\left(\frac{4\eta}{3} + \zeta\right)}{m_i n_{i0}\omega_{pi}a_i^2} \tag{25b}$$

where λ_i and a_i are the Debye length and mean interparticle distance for ions, respectively. The dependence of η^* on Γ_i is more complicated and cannot be expressed in a simple closed form. Numerically calculated values using codes (Ichimaru *et al.*, 1987) show that it is of order unity ($\approx$1.12) for values of Γ_i close to 1, goes to a minimum value ($\approx$0.06) for $\Gamma_i \approx 10$ and then monotonically increases for higher values of Γ_i.

Poisson's equation for the low-frequency part is given by

$$k^2\varphi_l = 4\pi e(Zn_{i1} - n_{el}). \tag{26}$$

Substituting the value of n_{el} and n_{i1} from Eqs. (18) and (23) in Eq. (26) we get

$$\varepsilon\varphi_l = -\chi_e\varphi_p, \tag{27}$$

where $\varepsilon = 1 + \chi_i + \chi_e$.

Using Eq. (9), the continuity equation for sidebands is given by

$$\frac{\partial n_{ea}}{\partial t} + n_{e0}i\vec{k}\cdot\vec{v}_{ea} + i\vec{k}\cdot\left(\frac{1}{2}n_{el}\vec{v}_{e0}^*\right) = 0, \tag{28}$$

$$\frac{\partial n_{eb}}{\partial t} + n_{e0}i\vec{k}\cdot\vec{v}_{eb} + i\vec{k}\cdot\left(\frac{1}{2}n_{el}\vec{v}_{e0}\right) = 0. \tag{29}$$

Using Eqs. (11), (28) and (ω_j, $\vec{k}$) (29), the linear density perturbations at the sidebands are given by

$$n_{ej}^L = \frac{k^2}{4\pi e}\chi_{ej}\varphi_j, \quad j = a, b, \tag{30}$$

where χ_{ej} is the electron susceptibility at sideband. One may write $\chi_{ej} = -(\omega_{pe}^2 + (3/2)k^2v_{th}^2)/\omega_j^2$. The non-linear density perturbations at ($\omega_{a,b}$, $\vec{k}$) due to the conjunction of density perturbation n_{el} with oscillatory velocity v_{e0} from Eqs. (28) and (29) are

$$n_{ea}^{NL} = \frac{\vec{k}\cdot\vec{v}_{e0}^*}{2\omega_a}n_{el} = \frac{\vec{k}\cdot\vec{v}_{e0}^*}{2\omega_a}\frac{k^2(1+\chi_i)\chi_e\varphi_p}{4\pi e\varepsilon}, \tag{31}$$

$$n_{eb}^{NL} = \frac{\vec{k}\cdot\vec{v}_{e0}}{2\omega_b}n_{el} = \frac{\vec{k}\cdot\vec{v}_{e0}}{2\omega_b}\frac{k^2(1+\chi_i)\chi_e\varphi_p}{4\pi e\varepsilon}. \tag{32}$$

The Poisson's equation for high-frequency sidebands is

$$k^2\varphi_{a,b} = -4\pi e(n_{ea,b}^L + n_{ea,b}^{NL}). \tag{33}$$

Using Eqs. (30)–(32) in Eq. (33), we obtain

$$\varepsilon_j\varphi_j = -4\pi e n_{ej}^{NL}/k^2, \quad j = a, b, \tag{34}$$

https://doi.org/10.1017/S0263034618000368 Published online by Cambridge University Press

where $\varepsilon_j = 1 + \chi_{ej} = 1 - (\omega_{pe}^2 + (3/2)k^2 v_{th}^2)/\omega_j^2$. Using Eqs. (27), (31) and (32) in Eq. (34) we get

$$\varphi_a = \frac{\vec{k}\cdot\vec{v}_{e0}^{*}}{2\omega_a\varepsilon_a}(1+\chi_i)\varphi_l, \tag{35}$$

$$\varphi_b = \frac{\vec{k}\cdot\vec{v}_{e0}}{2\omega_b\varepsilon_b}(1+\chi_i)\varphi_l. \tag{36}$$

Using Eqs. (15), (35) and (36) in Eq. (27), we finally obtain the dispersion relation for OTSI as

$$\varepsilon = -\chi_e(1+\chi_i)\frac{|\vec{k}\cdot\vec{v}_{e0}|^2}{4}\left(\frac{1}{\omega_a^2\varepsilon_a}+\frac{1}{\omega_b^2\varepsilon_b}\right). \tag{37}$$

Define a frequency mismatch $\Delta = \omega_0 - (\omega_{pe}^2 + (3/2)k^2 v_{th}^2)^{1/2}$ and substituting the value $\varepsilon_{a,b}$ and $\omega_{a,b}$ in Eq. (37), we can write the dispersion relation as

$$\varepsilon = -\chi_e(1+\chi_i)\frac{|\vec{k}\cdot\vec{v}_{e0}|^2}{4}\frac{\Delta}{\omega_0(\Delta^2-\omega^2)}. \tag{38}$$

Now using Eq. (38) we will study OTSI in two limits that is, kinetic limit where $\omega\tau_m > 1$ and the hydrodynamic limit where $\omega\tau_m < 1$. Here ω represents the frequency of the ion or the low-frequency mode. We first consider the kinetic regime.

Kinetic regime

In this regime $\omega\tau_m > 1$, we can write χ_e and χ_i from Eq. (24) as follows

$$\chi_e = \omega_{pi}^2/k^2C_{s0}^2,\ \ \chi_i = -\frac{\omega_{pi}^2}{\left[\omega^2 - \gamma_i\mu_i k^2 v_{thi}^2 - \frac{\eta^{*}\omega_{pi}k^2a_i^2}{\tau_m}\right]} \tag{39}$$

Using Eq. (25a) we can write Eq. (39) -

$$\chi_i = -\frac{\omega_{pi}^2}{\left[\omega^2 - (1+\frac{4}{15}u(\Gamma_i))k^2v_{thi}^2\right]} \tag{40}$$

On substituting these values in Eq. (38) we get a biquadratic equation of ω

$$(\omega^2-\Delta^2)\left(\omega^2 - \left(1+\frac{4}{15}u(\Gamma_i)\right)k^2v_{thi}^2 - \frac{\omega_{pi}^2}{\left(1+\frac{\omega_{pi}^2}{k^2C_{s0}^2}\right)}\right) = L\left(\omega^2 - \left(1+\frac{4}{15}u(\Gamma_i)\right)k^2v_{thi}^2 - \omega_{pi}^2\right)\Delta, \tag{41}$$

which can be simplified as

$$\omega^4 - \omega^2(\omega_{ac}^2 + \Delta^2 + L\Delta) + L\Delta\left(\omega_{pi}^2 + \left(1+\frac{4}{15}u(\Gamma_i)\right)k^2v_{thi}^2\right) + \Delta^2\omega_{ac}^2 = 0, \tag{42}$$

where

$$L = \frac{|v_{e0}|^2}{4C_{s0}^2}\frac{\omega_{pi}^2/\omega_0}{\left(1+\frac{\omega_{pi}^2}{k^2C_{s0}^2}\right)} \quad \text{and}$$

$$\omega_{ac}^2 = \left(1+\frac{4}{15}u(\Gamma_i)\right)k^2v_{thi}^2 + \frac{\omega_{pi}^2}{\left(1+\frac{\omega_{pi}^2}{k^2C_{s0}^2}\right)},$$

if we normalized ω by ω_{pi} Eq. (42) will be

$$\omega'^4 - \omega'^2(\omega_{ac}'^2 + \Delta'^2 + L'\Delta') + L'\Delta'\left(1+\left(1+\frac{4}{15}u(\Gamma_i)\right)\frac{T_i}{ZT_e}k^2\lambda_e^2\right) + \Delta'^2\omega_{ac}'^2 = 0, \tag{43}$$

where

$$\omega' = \frac{\omega}{\omega_{pi}},$$

$$\omega_{ac}'^2 = \left(1+\frac{4}{15}u(\Gamma_i)\right)\frac{T_i}{ZT_e}k^2\lambda_e^2 + \frac{1}{\left(1+\frac{1}{k^2\lambda_e^2}\right)},$$

$$L' = \frac{|v_{e0}|^2}{4C_{s0}^2}\frac{\omega_{pi}/\omega_0}{\left(1+\frac{1}{k^2\lambda_e^2}\right)},$$

$$\Delta' = \frac{\Delta}{\omega_{pi}} = \frac{\omega_0}{\omega_{pi}} - \left(\frac{\omega_{pe}^2}{\omega_{pi}^2} + \frac{m_i}{Zm_e}\frac{3}{2}k^2\lambda_e^2\right)^{1/2}.$$

The two roots of Equation (43) are

$$\omega'^2 = \frac{1}{2}\left[(\omega_{ac}'^2 + \Delta'^2 + L'\Delta') - \sqrt{(\omega_{ac}'^2 + \Delta'^2 + L'\Delta')^2 - 4\left(L'\Delta'\left(1+\left(1+\frac{4}{15}u(\Gamma_i)\right)\frac{T_i}{ZT_e}k^2\lambda_e^2\right) + \Delta'^2\omega_{ac}'^2\right)}\right]. \tag{44}$$

https://doi.org/10.1017/S0263034618000368 Published online by Cambridge University Press

Instability occurs when $\Delta^{'}$ <0 and

$$|\Delta'| < \frac{L'\left(1+\left(1+\frac{4}{15}u(\Gamma_i)\right)\frac{T_i}{ZT_e}k^2\lambda_e^2\right)}{\omega_{ac}'^2}.$$

If the two conditions given above are satisfied then the value of $\omega^{'2}$ will be negative which gives two imaginary roots, out of which one grows with time. This root corresponds to OTSI. Thus the growth rate of OTSI in the kinetic regime is

$$\frac{\gamma}{\omega_{pi}} = \left[\frac{1}{2}\left\{(\omega_{ac}'^2+\Delta'^2+L'\Delta') - \sqrt{(\omega_{ac}'^2+\Delta'^2+L'\Delta')^2 - 4\left(L'\Delta'(1+\left(1+\frac{4}{15}u(\Gamma_i)\right)\frac{T_i}{ZT_e}k^2\lambda_e^2) + \Delta'^2\omega_{ac}'^2\right)}\right\}\right]^{1/2}. \quad (45)$$

In the limit $\Gamma_i \to 0$ the growth rate in Eq. (45) reduces to the standard growth rate of OTSI (Ramachandran and Tripathi, 1997). In Figure 2, we have plotted the growth rate (γ) as a function of k for $\Gamma_i \approx 0$ (for the weak coupling limit) and for $\Gamma_i = 2.5$ and 5. The parameters which we have used in Figure 2 are as follows. Since OTSI takes place near the critical density (n_{cr}) region where $\omega_0 \approx \omega_{pe}$, we take $n_i \approx 10^{21}$ cm^{-3} ($n_e \approx n_{cr} \approx 10^{22}$ cm^{-3} for laser 351 nm), $T_e \approx 100-150$ eV, $T_i \approx 45-100$ eV, laser intensity(I) is10^{14}W/cm^2 and $Z = 5-10$ for Al ion plasma.

In the plot, we can see the growth rate increases with Γ_i. For example at $k \approx 0.6\times10^6$ cm^{-1}, the enhancement in the growth rate for $\Gamma_i = 2.5$ is about 25% and for $\Gamma_i = 5$ is about 40%. In Figure 3, we plot the growth rate (γ) as a function of normalized pump frequency (ω_0/ω_{pe}) for $k = 0.5\times10^6$ cm^{-1} with different $\Gamma_i \approx 0$, 2.5 and 5. OTSI will occur only when $\omega_0 \approx \omega_{pe}$. For higher values of ω_0, at which $\Delta^{'}$ becomes positive, OTSI will vanish. Next, we give a posterior justification for the kinetic regime condition $\gamma\tau_m$ >1. For particular values of plasma parameters ω_{pi}, λ_i and ion coupling parameter Γ_i, τ_m can be obtained from Eq. (25a).

So in Fig. 2 for $\Gamma_i = 2.5$, $\tau_m \approx 1.8\times10^{-11}$ s while the typical growth rate $\gamma \approx 0.45\times10^{13}$ s^{-1} and hence $\gamma\tau_m \approx 80$. Similarly for $\Gamma_i = 5$, $\tau_m \approx 2.7\times10^{-12}$ s and $\gamma\tau_m \approx 15$. Thus in Figure 2 and Figure 3, OTSI is indeed in the kinetic regime for $\Gamma_i = 2.5$ as well as for $\Gamma_i = 5$. It should be noted that since $\gamma \to 0$ as $k \to 0$, the growth rate must be chosen sufficiently away from zero for the kinetic regime to be valid.

Hydrodynamic regime

In this regime where $\omega\tau_m$ <1, χ_e and χ_i from Eq. (24) will be as follows

$$\chi_e = \omega_{pi}^2/k^2C_{s0}^2, \ldots \chi_i = -\frac{\omega_{pi}^2}{[\omega^2 - \gamma_i\mu_i k^2 v_{thi}^2]}. \quad (46)$$

On substituting these values in Eq. (38), the biquadratic equation which we obtain is

$$\omega'^4 - \omega'^2(\omega_{ac}'^2+\Delta'^2+L'\Delta') + L'\Delta'\left(1+\gamma_i\mu_i\frac{T_i}{ZT_e}k^2\lambda_e^2\right) + \Delta'^2\omega_{ac}'^2 = 0, \quad (47)$$

where

$$\omega' = \frac{\omega}{\omega_{pi}},$$

$$\omega_{ac}'^2 = \gamma_i\mu_i\frac{T_i}{ZT_e}k^2\lambda_e^2 + \frac{1}{\left(1+\frac{1}{k^2\lambda_e^2}\right)},$$

$$L' = \frac{|v_{e0}|^2}{4C_{s0}^2}\frac{\omega_{pi}/\omega_0}{\left(1+\frac{1}{k^2\lambda_e^2}\right)},$$

$$\Delta' = \frac{\Delta}{\omega_{pi}} = \frac{\omega_0}{\omega_{pi}} - \left(\frac{\omega_{pe}^2}{\omega_{pi}^2} + \frac{m_i}{Zm_e}\frac{3}{2}k^2\lambda_e^2\right)^{1/2}.$$

Two roots of Eq. (47) are-

$$\omega'^2 = \frac{1}{2}\left[(\omega_{ac}'^2+\Delta'^2+L'\Delta') - \sqrt{(\omega_{ac}'^2+\Delta'^2+L'\Delta')^2 - 4\left(L'\Delta'\left(1+\gamma_i\mu_i\frac{T_i}{ZT_e}k^2\lambda_e^2\right) + \Delta'^2\omega_{ac}'^2\right)}\right]. \quad (48)$$

For instability $\Delta^{'}$ must be negative and

$$|\Delta'| < \frac{L'\left(1+\gamma_i\mu_i\frac{T_i}{ZT_e}k^2\lambda_e^2\right)}{\omega_{ac}'^2}.$$

For the above two conditions, the value of $\omega^{'2}$ will be negative which further gives two imaginary roots and hence one of the roots of Eq. (48) gives the growth rate of OTSI in the hydrodynamic regime such that

$$\frac{\gamma}{\omega_{pi}} = \left[\frac{1}{2}\left\{(\omega_{ac}'^2+\Delta'^2+L'\Delta') - \sqrt{(\omega_{ac}'^2+\Delta'^2+L'\Delta')^2 - 4\left(L'\Delta'(1+\left(1+\gamma_i\mu_i\frac{T_i}{ZT_e}k^2\lambda_e^2\right)+\Delta'^2\omega_{ac}'^2\right)}\right\}\right]^{1/2}. \quad (49)$$

https://doi.org/10.1017/S0263034618000368 Published online by Cambridge University Press

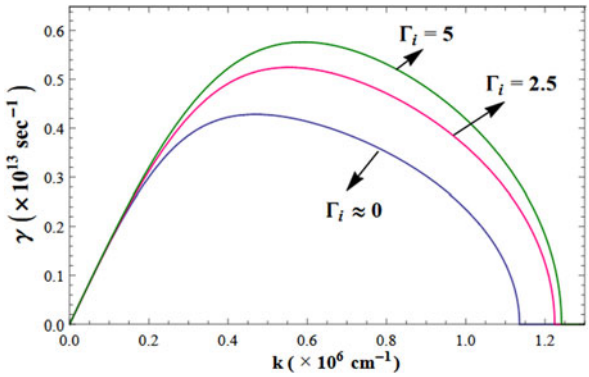


Fig. 2. Variation in growth rate (γ) as a function of k for $\Gamma_i = 2.5$ and $\Gamma_i = 5$ in the kinetic regime. The case of $\Gamma_i \approx 0$ is included for comparison with weak coupling limit ($\Gamma_i < 1$).

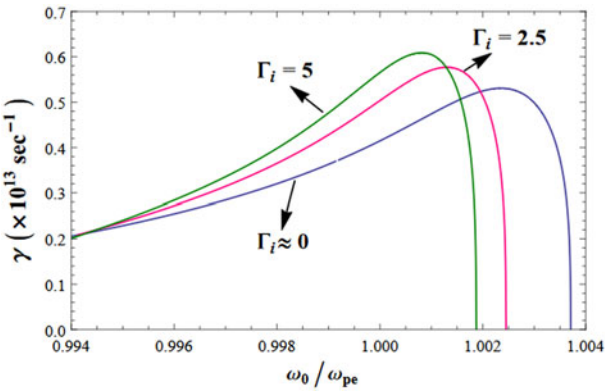


Fig. 3. Variation in growth rate (γ) as a function of ω_0/ω_{pe} for $k = 0.5 \times 10^6\ \mathrm{cm}^{-1}$ with different values of Γ_i in the kinetic regime. The case of $\Gamma_i \approx 0$ is included for comparison with weak coupling limit ($\Gamma_i < 1$).

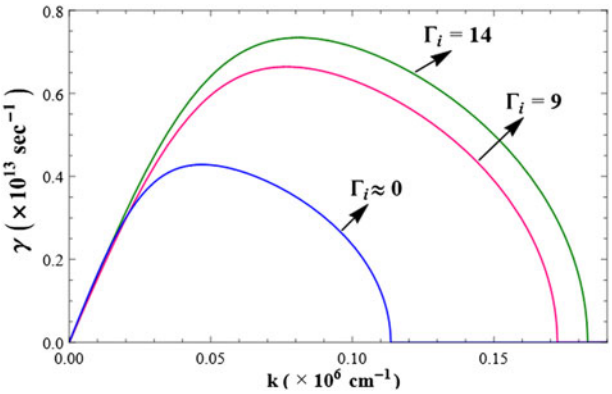


Fig. 4. Variation in growth rate (γ) as a function of k for $\Gamma_i = 9$ and $\Gamma_i = 14$ in the hydrodynamic regime. The case of $\Gamma_i \approx 0$ is included for comparison with weak coupling limit ($\Gamma_i < 1$).

The growth rate in Eq. (49) reduces to the standard growth rate of OTSI in the limit $\Gamma_i \to 0$. In Figure 4 we have plotted the growth rate (γ) as a function of k for $\Gamma_i = 9$ and $\Gamma_i = 14$, where the laser intensity (I) is $10^{14}\mathrm{W/cm}^2$, $n_e \approx 10^{22}\ \mathrm{cm}^{-3}$, $T_e \approx 75$ eV, $T_i = 20 - 25$ eV, $Z = 10$–11 (for Al ion) and $\omega_0 \approx \omega_{pe}$. The curve $\Gamma_i \approx 0$ shows the growth rate in weakly coupled plasma.

The plot shows a large increment in the growth rate of OTSI (by almost 200%) for $k = 1 \times 10^6 \mathrm{cm}^{-1}$ and $\Gamma_i = 14$. For $\Gamma_i = 9$ the enhancement in the growth rate at $k = 1 \times 10^6\ \mathrm{cm}^{-1}$ is about 160%. Thus the destabilization effect of strongly coupled ions is much severe in the hydrodynamic limit than in the kinetic limit. To give a posterior justification for the hydrodynamic regime condition $\gamma\tau_m < 1$, we find for $\Gamma_i = 9$, $\tau_m \approx 0.3 \times 10^{-13}$ s while the typical growth rate $\gamma \approx 0.6 \times 10^{13}\ \mathrm{s}^{-1}$ and hence $\gamma\tau_m \approx 0.1$, similarly for $\Gamma_i = 14$, $\tau_m \approx 0.9 \times 10^{-14}$ s and $\gamma\tau_m \approx 0.06$. Hence in Figure 4, OTSI is in the hydrodynamic regime for $\Gamma_i = 9$ as well as for $\Gamma_i = 14$.

Summary and discussions

In this paper, we have studied the OTSI in the presence of strongly coupled ions. The situation involving strongly coupled ions is likely to arise in a number of cases. For example in the case of Au blow of plasma near the hohlraum wall in the indirect drive experiments in ICF scheme, the gold ions may become strongly coupled due to large electronic charge. In case of the direct drive approach, the carbon ions of the ablator material in the coronal plasma may become strongly coupled. Similarly, in the case of laser-driven ion accelerator, a pre-plasma of C or Al ions is formed on the target's front side, where the density of plasma is near critical density. In this region, C or Al ions may become strongly coupled. Typically in these situations, the ion correlation factor Γ_i can be as high as 2–15. In this regime, the ion behaves as strongly coupled viscoelastic fluid. The strong coupling effects are included here *via* GHD equation. It is shown that in a typical parameter regime of OTSI, these strong correlation effects modify the compressibility $\mu_i(\Gamma_i)$. This can be integrated once to give the ion pressure P_i as a function of Γ_i given by the expression $P_i = (0.73 - 0.3\Gamma_i + 0.31\Gamma_i^{1/4} + 0.07\Gamma_i^{-1/4})n_i T_i$. As can be seen from this expression with increasing Γ_i ion pressure decreases and for $\Gamma_i > 4$ it becomes negative. We have examined the effects of strong correlation in the two regimes that is, the kinetic regime (valid for $\omega\tau_m > 1$) and the hydrodynamic regime (valid for $\omega\tau_m < 1$). Our results show that these strong correlation effects lead to significant enhancement of the growth rate of OTSI. This destabilization is caused by enhancing bunching of ions due to its negative pressure as shown in Figure 1.

It should be noted that extreme compression also leads to plasma electrons and ions correlation. Strong correlations generated due to high compression cannot be described by GHD theory (Avinash, 2015). These effects may also become significant in laser fusion targets and ion acceleration which will be the subject of future publication.

Acknowledgement. This research was supported by the Board of Research in Nuclear Sciences (BRNS), Department of Atomic Energy, Government of India (Grant No. 39/14/24/2016-BRNS/34177). One of the authors (P.S.) acknowledges the financial support from the University Grants Commission (UGC), India, under the SRF scheme.

References

Avinash K (2015) Theory of correlation effects in dusty plasmas. *Physics of Plasmas* **22**, 033701.

Berkovsky MA (1992) Spectrum of low frequency modes in strongly coupled plasmas. *Physics Letters A* **166**, 365.

Boon JP and Yip S (1980) *Molecular Hydrodynamics*. NewYork: McGraw-Hill.

https://doi.org/10.1017/S0263034618000368 Published online by Cambridge University Press

Chen FF (1985) *Introduction to Plasma Physics and Controlled Fusion*. New York: Plenum, pp. 309–322.

Craxton RS, Anderson KS, Boehly TR, Goncharov VN, Harding DR, Knauer JP, McCrory RL, McKenty PW, Meyerhofer DD, Myatt JF, Schmitt AJ, Sethian JD, Short RW, Skupsky S, Theobald W, Kruer WL, Tanaka K, Betti R, Collins TJB, Delettrez JA, Hu SX, Marozas JA, Maximov AV, Michel DT, Radha PB, Regan SP, Sangster TC, Seka W, Solodov AA, Soures JM, Stoeckl C and Zuegel JD (2015) Direct-drive inertial confinement fusion: A review. *Physics of Plasmas* **22**, 110501.

Das A and Kaw P (2014) Suppression of Rayleigh Taylor instability in strongly coupled plasmas. *Physics of Plasmas* **21**, 062102.

Esirkepov TZh, Koga JK, Sunahara A, Morita T, Nishikino M, Kageyama K, Nagatomo H, Nishihara K, Sagisaka A, Kotaki H, Nakamura T, Fukuda Y, Okada H, Pirozhkov A, Yogo A, Nishiuchi M, Kiriyama H, Kondo K, Kando M and Bulanov SV (2014) Prepulse and amplified spontaneous emission effects on the interaction of a petawatt class laser with thin solid targets. *Nuclear Instruments & Methods in Physics Research, Section A: Accelerators, Spectrometers, Detectors, and Associated Equipment* **745**, 150.

Fernandez JC, Cobble JA, Failor BH, Dubois DF, Montgomery DS, Rose HA, Vu HX, Wilde BH, Wilke MD and Chrien RE (1996) Observed dependence of stimulated Raman scattering on ion-acoustic damping in hohlraum plasmas. *Physical Review Letters* **77**, 2702.

Frenkel YI (1946) *Kinetic Theory of Liquids*. Oxford: Clarendon.

Fried BD, Kemura TI, Nishikawa K and Schmidt G (1976) Parametric instabilities with finite wavelength pump. *Physics of Fluids* **19**, 1975.

Ichimaru S, Iyetomi H and Tanaka S (1987) Statistical physics of dense plasmas: Thermodynamics, transport coefficients and dynamic correlations. *Physics Reports* **149**, 91.

Janaki MS, Chakrabarti N and Banerjee D (2011) Jeans instability in a viscoelastic fluid. *Physics of Plasmas* **18**, 012901.

Kaw PK and Sen A (1998) Low frequency modes in strongly coupled dusty plasmas. *Physics of Plasmas* **5**, 3552.

Kirkwood RK, Macgowan BJ, Montgomery DS, Afeyan BB, Kruer WL, Moody JD, Estabrook KG, Back CA, Glenzer SH, Blain MA, Williams EA, Berger RL and Lasinski BF (1996) Effect of ion-wave damping on stimulated Raman scattering in high-z laser-produced plasmas. *Physical Review Letters* **77**, 270.

Kumar S and Malik HK (2006) Effect of negative ions on oscillating two stream instability of a laser driven plasma beat wave in a homogeneous plasma. *Physica Scripta* **74**, 304.

Lindl JD, Amendt P, Berger RL, Glendinning SG, Glenzer SH, Haan SW, Kauffman RL, Landen OL and Suter LJ (2004) The physics basis for ignition using indirect-drive targets on the National Ignition Facility. *Physics of Plasmas* **11**, 339.

Lindl J, Landen O, Edwards J and Moses E & NIC Team (2014) Review of the National Ignition Campaign 2009–2012. *Physics of Plasmas* **21**, 020501.

Liu CS and Tripathi VK (1995) *Interaction of Electromagnetic Waves with Electron Beams and Plasmas*, Chaps.4 and 7. Singapore: World Scientific.

Malik HK (2007) Oscillating two stream instability of a plasma wave in a negative ion containing plasma with hot and cold positive ions. *Laser and Particle Beams* **25**, 397.

Malik HK and Singh S (2011) Conditions and growth rate of Rayleigh instability in a Hall thruster under the effect of ion temperature. *Physical Review E* **83**, 036406.

Malik OP, Singh S, Malik HK and Kumar A (2015*a*) High-frequency instabilities in an explosion-generated relativistic plasma. *Journal of Theoretical and Applied Physics* **9**, 105.

Malik OP, Singh S, Malik HK and Kumar A (2015*b*) Low and high frequency instabilities in an explosion-generated-plasma and possibility of wave triplet. *Journal of Theoretical and Applied Physics* **9**, 75.

Mulser P, Giulietti A and Vaselli M (1984) Quantitative explanation of oscillating two-stream and parametric decay instabilities in terms of wave pressure. *Physics of Fluids* **27**, 2035.

Murillo MS (1998) Static local field correction description of acoustic waves in strongly coupling dusty plasmas. *Physics of Plasmas* **5**, 3116.

Nicholson DR (1981) Oscillating two-stream instability with pump of finite extent. *Physics of Fluids* **24**, 908.

Ramachandran K and Tripathi VK (1997) Oscillating two-stream instability of a plasma wave in a plasma channel. *IEEE Transactions on Plasma Science* **25**, 423.

Rosenbluth MN (1972) Parametric Instabilities in Inhomogeneous Media. *Physical Review Letters* **29**, 565.

Satya YS, Jain KM, Guha S and Bose M (1985) Low-frequency modes in a two-species plasma. *Journal of Plasma Physics* **34**, 247.

Sharma P, Avinash K and Gupta DN (2016) Parametric instabilities in strongly correlated plasma. *Physics of Plasmas* **23**, 102704.

Singh S, Malik HK and Nishida Y (2013) High frequency electromagnetic resistive instability in a Hall thruster under the effect of ionization. *Physics of Plasmas* **20**, 102109.

Slattery WL, Doolen GD and DeWitt HE (1980) Improved equation of state for the classical one-component plasma. *Physical Review A* **21**, 2087.

Slattery WL, Doolen GD and DeWitt HE (1982) N dependence in the classical one-component plasma Monte Carlo calculations. *Physical Review A* **26**, 2255.

Snavely RA, Key MH, Hatchett SP, Cowan TE, Roth M, Phillips TW, Stoyer MA, Henry EA, Sangster TC, Singh MS, Wilks SC, MacKinnon A, Offenberger A, Pennington DM, Yasuike K, Langdon AB, Lasinski BF, Johnson J, Perry MD and Campbell EM (2000) Intense high-energy proton beams from petawatt-laser irradiation of solids. *Physical Review Letters* **85**, 2945.

Tyagi J, Singh S and Malik HK (2018) Effect of dust on tilted electrostatic resistive instability in a Hall thruster. *Journal of Theoretical and Applied Physics* **12**, 39.

Weaver JL, Oh J, Afeyan B, Phillips L, Seely J, Feldman U, Brown C, Karasik M, Serlin V, Aglitskiy Y, Mostovych AN, Holland G, Obenschain S, Chan L-Y, Kehne D, Lehmberg RH, Schmitt AJ, Colombant D and Velikovich A (2007) Laser plasma instability experiments with KrF lasers. *Physics of Plasmas* **14**, 056316.

Wilks SC, Langdon AB, Cowan TE, Roth M, Singh M, Hatchett S, Key MH, Pennington D, MacKinnon A and Snavely RA (2001) Energetic proton generation in ultra-intense laser–solid interactions. *Physics of Plasmas* **8**, 542.

Yadav S, Tripathi VK and Gupta VL (2003) Stimulated Brillouin scattering of a laser in a high-*Z* plasma channel embedded with light ions. *Physica Scripta* **68**, 66.

Yadav S, Gupta DN, Tripathi VK and Gupta VL (2004) Oscillating two stream instability of a laser in a two ion species plasma. *Physica Scripta* **69**, 130.

https://doi.org/10.1017/S0263034618000368 Published online by Cambridge University Press